TESTS OF THE TULLY-FISHER RELATION. II. SCATTER USING OPTICAL ROTATION CURVES[1]

SOMAK RAYCHAUDHURY

Inter-University Centre for Astronomy and Astrophysics, Pune 411 007, India
Electronic mail: somak@iucaa.ernet.in

KASPAR VON BRAUN AND GARY M. BERNSTEIN

Department of Astronomy, University of Michigan, 830 Dennison Building, Ann Arbor, Michigan 48109
Electronic mail: kaspar, garyb@astro.lsa.umich.edu

PURAGRA GUHATHAKURTA

UCO/Lick Observatory, University of California, Santa Cruz, California 95064
Electronic mail: raja@ucolick.org
Received 1997 January 14; revised 1997 March 14

ABSTRACT

We investigate the amount of scatter in the Tully-Fisher relation (TFR) when using optical long-slit $H\alpha$ rotation curves to determine the velocity widths of spiral galaxies. We study a sample of 25 galaxies in the Coma region of the sky which were shown in Bernstein *et al.* (1994, AJ, 107, 1962) to exhibit an extraordinarily low scatter of 0.10 mag rms in the *I* magnitude vs 21-cm width TFR. Using the same *I* magnitudes with new widths derived from high-quality $H\alpha$ rotation curves, we measure an rms scatter of 0.14 mag in the TFR. This suggests that measurement errors and ''astrophysical errors'' (such as non-circular gas motion) on the $H\alpha$ velocity widths are below 6%, and optical widths are nearly as good for TFR studies as 21-cm widths. The scatter and form of the TFR are found to be robust under choice of velocity width-extraction algorithm, as long as the central portions of the optical rotation curve are ignored and low-S/N points are not weighted too heavily. In this small sample there is no evidence that rotation curve shapes vary systematically with rotation velocity, nor that rotation curve shape can be used to reduce the scatter in the TFR. © *1997 American Astronomical Society.* [S0004-6256(97)02906-3]

1. INTRODUCTION

Peculiar velocity surveys of thousands of spiral galaxies are now being conducted using the Tully-Fisher relation (TFR, Tully & Fisher 1977) between the speed of rotation of a spiral and its absolute magnitude. The majority of these surveys have been conducted using 21-cm H I rotation widths, but many now also make use of long-slit optical $H\alpha$ rotation curves to determine the rotation speed (e.g., Mathewson *et al.* 1992; Giovanelli *et al.* 1997a, 1997b; Willick *et al.* 1996).

In this paper we ask how the scatter in the TFR using optical data compares to the 21-cm TFR scatter. This comparison is facilitated by the use of a sample of 25 galaxies in the Coma Supercluster region which we have previously shown to have extraordinarily low scatter in the *I* magnitude vs 21-cm width TFR—only 0.10 mag rms (Bernstein *et al.* 1994, hereafter referred to as Paper I). We have obtained high-quality $H\alpha$ rotation curves for all these galaxies, have extracted velocity widths, and determined the TFR scatter using optical widths. Since the photometry and 21-cm data for these galaxies (either by chance or for some not-yet-

understood physical reason) give a nearly perfect 21-cm TFR, we are able to perform a very sensitive test for additional scatter induced in the TFR by a switch from 21 cm to $H\alpha$ linewidths. The scatter in the optical TFR will present an upper limit on the TFR scatter associated with the optical widths, whether the cause be measurement error or some failure of the rotation curves to reflect the ''true'' rotation width.

2. EXPECTATIONS AND PREVIOUS RESULTS

A priori, 21-cm widths are expected to be superior to optical widths in the context of TFR studies. The detectable 21-cm emission extends further out into the disk of the spiral than the $H\alpha$ emission, and the gas motions are likely more regular and circular in the outer disk than in the central sections. The 21-cm velocity should then better reflect the presumed underlying physical variable of the TFR, galaxy mass, and thus produce lower TFR scatter. Secondly, all H I atoms in the galaxy contribute equally to the 21-cm profile (dubbed ''atomic democracy'' by Schommer *et al.* 1993) so the data are not biased or restricted to areas of high ultraviolet radiation. Furthermore, 21-cm signals are not attenuated by dust—though extinction of $H\alpha$ photons is relatively small at 2–3 scale lengths into the disk where the most relevant dy-

---

namical information lies. Finally, it is easy to achieve <10 km s^{-1} resolution in 21-cm observations.

Long-slit rotation curves have the advantage over 21-cm profiles of being a two-dimensional data set (spatial and velocity axes). The latter have no spatial information, so it is not possible to distinguish thermal or non-circular motions from true rotation. On the long-slit rotation curve, random motions appear as noise atop the true rotation and thus can be removed. In choosing an algorithm to extract a single rotation width from the rotation curve, we may also restore some "atomic democracy" if we do not place too much weight on H II regions with high flux, even though such regions might have very small formal errors on the recession velocity. Furthermore, the morphology of the rotation curve could provide extra information to help reduce TFR scatter.

It is also possible to obtain three-dimensional data (two spatial axes and one velocity axis) using Fabry-Perot images of the Hα emission, as demonstrated by Schommer *et al.* (1993). In theory this extra information should help detect dynamical irregularities even better than long-slit data, and also allows determination of the galaxy inclination and position angle independent of the photometric data. By simulating long-slit observations of their Fabry-Perot datacubes, Schommer *et al.* demonstrate several potential problems for long-slit measurements. They conclude, however, that for highly inclined galaxies differences between Fabry-Perot and long-slit estimates of the rotation speed will be small.

Long-slit Hα measurements are perhaps the easiest to make in practice. They certainly require less telescope time than Fabry-Perot measurements, and can be extended to much more distant galaxies than 21-cm methods—especially in regions of the sky which are inaccessible to the Arecibo telescope. Rotation curves of spirals at 7000 km s^{-1} recession velocity can be obtained in under an hour with 2-meter class optical telescopes, but become difficult to observe with radio telescopes other than Arecibo. Of course a practical disadvantage to long-slit observations is that one must know the position angle of the galaxy dynamical major axis in advance (preferably to an accuracy of 2°–3°). In our study the photometric position angle is known to 1°–2° because we precede the Hα observations with very deep *I*-band imaging, and we remove from our sample any galaxy in which the outer isophotes twist by more than a few degrees. It has been noted (Franx & de Zeeuw 1992) that if spiral disks are not intrinsically round, then the photometric major axis will not in general coincide with the dynamical major axis, causing errors in long-slit observations. Our optical TFR scatter may be taken as a test of this non-circularity.

These practical considerations have led others to attempt TFR measurements with optical rotation curves. Courteau (1992) conducted a TFR peculiar velocity survey with Hα rotation widths, and investigated several algorithms for extracting a width W from a rotation curve. These are evaluated first by checking variations on repeat measurements, and also by comparison with 21-cm values. As one might expect, algorithms which involve choosing a maximum point on each arm of the rotation curve fare poorly because they will usually extract the width from the noisiest bins. The lowest internal scatter in W (10 km s^{-1}) results from essentially averaging all velocities over each arm of the rotation curve. Courteau chose, however, to add all the spectra along the slit, discarding all spatial information, and collapsing all the Hα flux into a single velocity profile. He then derived W by means similar to those used for 21-cm profiles. While his spatially-averaged optical widths gave higher internal errors (12–13 km s^{-1}) than W estimates which use the spatial information in the rotation curve, the offset from 21-cm W's is smaller, which made them better suited to his purposes.

Other investigators have used Hα rotation curves to obtain W but do not explicitly compare various algorithms. Mathewson *et al.* (1992) subtract the minimum from the maximum of the rotation curve to obtain W, and measure an internal scatter of 10 km s^{-1}. As discussed below, it is likely that they have enforced some unspecified minimum S/N on the rotation curve points. Giovanelli *et al.* (1997a, 1997b) reinterpret some of the Mathewson, Ford, and Buchhorn rotation curves by defining W to be the width at R_{opt} (the 83%-light radius) from the galaxy center. This requires extrapolation for some rotation curves which do not reach this deep into the disk (3.2 scale lengths).

Vogt (1994) extracted widths from rotation curves using a variant of the velocity-profile method: she measured the mean velocity in each spatial bin along the rotation curve, ranked these velocities in order, and defined the rotation width to be the difference between the 10th and 90th percentile points of the velocity distribution. This should encourage more atomic democracy than the Courteau algorithm, because it weights all parts of the rotation curve equally rather than by flux.

3. MEASUREMENTS OF ROTATION CURVES

3.1 The Sample

The Coma Supercluster galaxy sample and the collection of photometric data are described in Paper I. Briefly, we select those galaxies within a few degrees of the Coma cluster core, with recession velocities in the range 5000–8000 km s^{-1}, for which 21-cm profiles could be found in the literature. Deep *I*-band surface photometry was obtained for each galaxy. We discarded galaxies for which the ellipticity varied by more than 0.03 across the outer isophotes or for which the position angle twisted by more than $\approx 3°$—e.g., those with tidal tails, those for which the isophotal shape was dominated by the spiral arms, or those with morphological peculiarities. For these discarded galaxies ($\sim 15\%$ of the full sample), we have little confidence that the isophotal shape accurately reflects the disk inclination, making it difficult to derive the rotation speed from line-of-sight velocities along the photometric major axis. We also removed from the sample those galaxies ($\sim 6\%$ of the full sample) for which the 21-cm profile did not have sufficiently steep sides to obtain a reliable width.

In Paper I we demonstrate that few (if any) of the galaxies in our sample are likely to be members of the Coma cluster itself, and we henceforth assume that their distances are proportional to their redshifts.

3.2 Observations

Each of the galaxies was observed in 1993 March or 1993 June using the Red Channel spectrograph on the Multiple Mirror Telescope (effective aperture of 4.5 m). A 1200 lines mm^{-1} grating blazed at 575 nm gives a resolution of ~0.21 nm per pixel near the Hα line. In addition, the thinned 800×1200 CCD was binned to $0\overset{''}{.}6$ pixels in the spatial direction. The slit dimensions were $1\overset{''}{.}25\times180''$, with the width chosen to admit as much light as possible without significantly degrading the spectral resolution. Most of the galaxies were observed for a single 1200 s exposure, with some of the fainter galaxies observed for two 1200 s exposures. This is significantly deeper than most existing TFR rotation curve studies—we wish to investigate the "intrinsic" errors in the TFR using rotation curves rather than have the scatter be dominated by errors from photon noise. Position angles for the galaxies were chosen to match the outer isophotes of the I-band images. Galaxy nuclei were centered on the slit using the MMT guiding camera.

The galaxy observations were interspersed with short wavelength calibration exposures of a He-Ne-Ar arc lamp, and quartz lamp flat-field exposures. Quartz lamp spectra were also obtained through a "decker" slit consisting of a row of small holes. Long-slit spectra of the twilight sky were also obtained.

3.3 Extraction of Rotation Curves

Each galaxy exposure was flat-fielded using the quartz lamp exposure adjacent in the observing sequence, and a wavelength solution for the entire CCD was derived from the adjacent He-Ne-Ar arc lamp exposure. Residuals to the wavelength fit are typically 0.005 nm. Twilight exposures were used to compensate for slight differences (dependent on the position of the slit) between lamp throughput and sky throughput caused by small differences between the pupil illumination by the lamp and by the sky. Finally, the decker slit quartz lamp exposures were used to map the distortion of the spatial coordinate on the chip. Thus for each exposure we produce a map from pixel coordinates (x,y) to (s,λ) space (slit position vs wavelength).

For a given pixel corresponding to (s_i,λ_j), we determined the sky background as follows: we determined the flux at λ_j for each other row (s value) in the image. Note that since the spectrum is tilted relative to pixel coordinates, this may require interpolation. We then fit a linear function of s to the derived sky background intensity vector, omitting of course the central parts of the slit over which the galaxy emission can be seen on the CCD image.

Cosmic rays were identified by eye, and the IRAF task IMEDIT was used to linearly interpolate over pixels affected by cosmic rays. Each pixel was then assigned to a bin according to its spatial coordinate s. Bin widths were 3 to 10 pixels ($1\overset{''}{.}8-6''$) depending upon the S/N of the emission lines. Within each spatial bin, the intensities in each spectral pixel were fit to a model function of wavelength λ which includes continuum radiation and gaussian profiles for the Hα and the two [N II] lines (undersampling of the spectral line profile is accounted for). Each spectral line was allowed

to have an independent intrinsic width (which was then convolved with the instrumental width) and flux, but the three lines were constrained to have the same recession velocity. Thus for a linear background, the spectral model has 2 parameters for continuum, 6 line strength/width parameters, and one velocity parameter. This model was fit to an ≈80-pixel (~17 nm) segment of the spectrum spanning the Hα and [N II] lines, leaving ≈70 DOF for the fit. Chi-squared values were typically 70–100, except near the galaxy nucleus, where the continuum has high enough S/N to make the linear approximation inadequate. Note that we *do not rebin or interpolate* the spectra.

The fitting process resulted in an estimate of recession velocity v_i and its uncertainty σ_{v_i} for each bin, with the bins centered at positions s_i along the slit. We only used bins in which the Hα emission was detected at S/N>3.5, which leads to velocity uncertainties smaller than 12 km s^{-1} even in the noisiest parts of the rotation curves. Rotation curves for the 25 galaxies are shown in Fig. 1.

4. VELOCITY WIDTH ALGORITHMS

We must extract a single width W from the rotation curves in order to produce a TFR. Desirable qualities for the W measurement algorithm are:

(1) The resultant W should be robust under changes in binning of the rotation curve data (or changes in spatial resolution).

(2) W should also vary little with the S/N level of the observations.

(3) W should have minimum variance for repeat observations at a given S/N level of the spectrum.

(4) The algorithm should try to promote "atomic democracy" (see Sec. 2).

(5) The algorithm should not make *a priori* assumptions about the shape of the rotation curve.

(6) Most importantly, it should minimize the scatter in the TFR.

The first three of these criteria lead us to design algorithms that use as much of the rotation curve as possible in some form of averaging or fitting process—though criterion (5) leads us to avoid fitting functional forms to the curves. Choosing the maximum and minimum velocity of the rotation curves (and subtracting to get W) is a very poor method, because the final W is determined by the noisiest bins. The derived W will have a strong tendency to increase as S/N worsens or spatial bin size is decreased. We describe here several width-determination algorithms which we apply to the data in order to see which performs best under criterion (6), minimal TFR scatter.

4.1 Min-Max Method

This is the "straw man" method upon which we hope to improve. The width W is simply $v_{max}-v_{min}$, where v_{max} and v_{min} are the maximum and minimum of the v_i. This indeed leads to quite undesirable results, with a TFR scatter of 0.4 mag. The noise in the estimate of W is much abated if we consider only those v_i for which the Hα line has S/N>3.5 and $\sigma_{v_i}<12$ km s^{-1}; we will henceforth retain this restric-
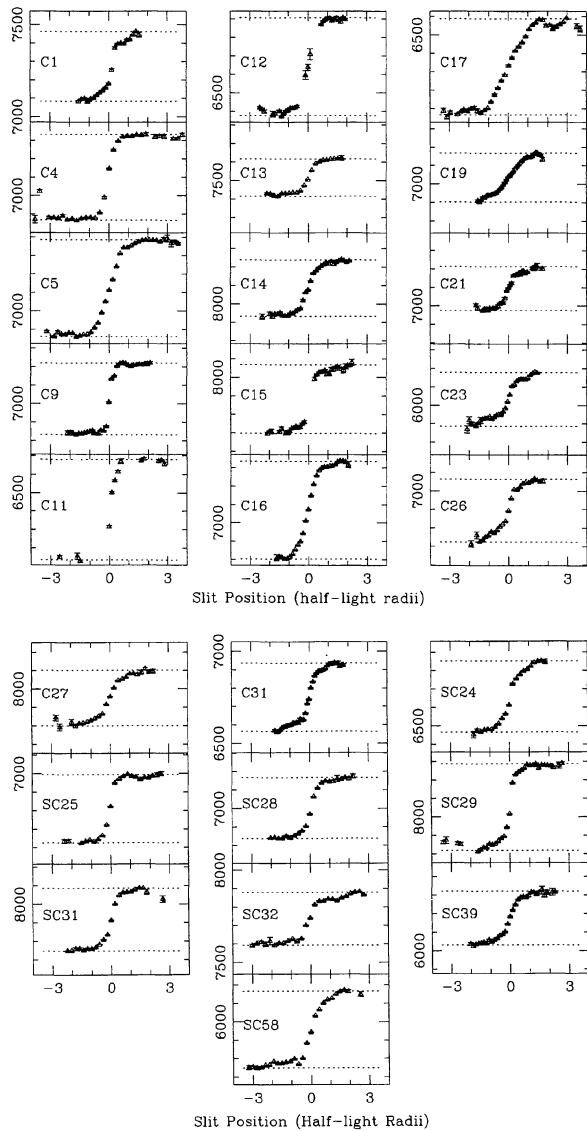
FIG. 1. Rotation curves for the 25 galaxies in the sample. Bins with S/N below 3.5 are omitted. The x axis is in units of each galaxy's half-light radius $r_{1/2}$, and the y axis is recession velocity in km s^{-1}. All galaxies are on a common scale with each vertical tick being 100 km s^{-1}. Dashed lines are the velocities of the two arms as determined by the Probable Min-Max method.

tion. Some form of this algorithm is used by Mathewson *et al.* (1992), and Courteau (1992) also experiments with variants of this method. The "percentile" method of Vogt (1994)—choosing the width to be the difference between the 10th and 90th percentile points of the velocity histogram—is similar to the min-max method, but with much reduced sensitivity to the noise level. Vogt also reduces sensitivity to noise by using only points with small uncertainties.

4.2 Weighted Mean Method: Entire Side

The width W is here defined to be $|v_{left} - v_{right}|$, where the left and right side velocities are the weighted averages of the entire side of the rotation curve. The center is located at the

maximum of the continuum flux. The velocity data points are weighted by $\sigma_{v_i}^{-2}$ as usual; this might subvert "atomic democracy" by weighting too heavily those bright H II regions with high flux and thus low σ_{v_i}. We could encourage atomic democracy by replacing σ_v by some minimum value (≈ 1 km s^{-1}) if the flux is high enough to make the formal error smaller. For our sample, however, we find that this does not make a significant difference for any of the weighted mean algorithms considered.

4.3 Weighted Mean Method: Outer Segments

This algorithm is the same as the previous algorithm, except that the inner part of the rotation curve is not used in calculating the weighted means. We define $s = 0$ to be the center of the rotation curve, and the extent S of each side of the rotation curve is defined by outermost s_i which satisfies the S/N limit. We then perform a weighted mean on each side for all points with $S/2 < s_i < S$. Courteau (1992) obtains his best internal consistency with a similar algorithm.

4.4 Weighted Mean Method: Half-light Radii

We improve upon the "outer segments" algorithm by averaging the v_i (taking a weighted mean) over an interval in s located a fixed number of half-light radii from the center of the galaxy. Half-light radii $r_{1/2}$ (actually half-light semi-major axes) are determined from the I-band photometry and thus, unlike the "lengths" of the rotation curves above, are independent of galaxy distance or rotation curve S/N. We define the velocity of each arm to be the weighted mean over the range $[r_{1/2}, 2r_{1/2}]$. We also calculate widths using the range $[r_{1/2}, 4r_{1/2}]$. For comparison we note that an exponential disk galaxy has $r_{1/2}$ equal to 1.68 scale lengths, and also has $r_{1/2} = 0.52R_{opt}$, where R_{opt} is the 83%-light radius defined by Persic *et al.* (1996, hereafter referred to as PSS96).

4.5 Fixed-Point Method

We measure the velocity of each arm of the rotation curve at a fixed number of half-light radii from the center. The v_i are interpolated to the appropriate point; only points with S/N>3.5 are used for interpolation. We find that the lowest scatter is obtained by choosing the fixed point at $1.3r_{1/2}$ from the center, though the TFR scatter depends only weakly upon the exact choice as long as the fixed point is beyond $r_{1/2}$. Giovanelli *et al.* (1997b), for example, choose to measure W at $R_{opt} = 1.9r_{1/2}$. We choose not to use such a large radius because for a few of our galaxies (and those of Mathewson *et al.* 1992 which Giovanelli *et al.* use), this requires extrapolation past the high-S/N region of the rotation curve.

4.6 Probable Min-Max Method

The above algorithms determine some average rotation velocity, or velocity on a robustly determined section of the rotation curve. It may be that the TFR is tighter when W is a measure of the maximum rotation speed of the galaxy instead of some average rotation speed. Unfortunately, a simple maximum of the v_i is not robust (Sec. *4.1*). Here we

TABLE 1. Galaxy data.

Code	Name	I' [mag]	e	PA [°]	$r_{1/2}$ ["]	v [km s^{-1}]	W (Hα) [km s^{-1}]	W (Hα) [km s^{-1}]	W (21-cm) [km s^{-1}]	f
(1)	(2)	(3)	(4)	(5)	(6)	(7)	(8)	(9)	(10)	(11)
SC24	128-087	13.16	0.73	80	16.5	6672	384	354	404	0.73
SC25	158-105	13.03	0.62	−79	13.9	6821	370	342	393	0.85
SC28	129-010	13.51	0.74	27	14.9	7016	330	312	366	0.77
SC31	99-104	13.77	0.70	12	14.7	7934	339	328	382	0.74
SC32	159-055	14.07	0.72	74	13.0	7750	285	234	318	0.71
SC39	159-096	13.52	0.64	8	22.3	6189	292	274	313	0.71
SC58	131-008	13.16	0.79	38	14.0	5981	408	363	434	0.71
C1	160-088	12.81	0.50	55	19.4	7287	377	364	391	0.74
C4	160-102	12.78	0.71	88	12.7	7103	464	451	498	0.80
C5	130-012	12.65	0.81	−38	16.0	7130	526	495	554	0.67
C9	160-137	12.17	0.43	−39	12.8	7030	388	372	459	0.88
C11	160-166	11.64	0.44	22	20.1	6411	542	537	567	0.68
C12	160-192	12.07	0.61	−78	26.7	6648	518	509	564	0.72
C13	159-059	13.64	0.30	24	9.4	7519	202	190	216	0.77
C14	159-082	13.21	0.38	11	13.7	8087	305	290	321	0.73
C15	159-099	13.75	0.70	−86	17.0	7886	372	341	392	0.78
C16	159-102	12.52	0.70	34	13.2	7071	529	509	551	0.74
C17	159-110	12.48	0.79	72	17.2	6330	522	458	541	0.56
C19	UGC8195	14.47	0.86	89	20.8	7038	263	227	268	0.65
C21	UGC8244	14.07	0.62	78	20.8	7099	237	226	269	0.72
C23	160-167	13.31	0.56	−43	15.7	6035	293	270	308	0.66
C26	159-080	13.59	0.73	7	12.3	6897	342	306	360	0.74
C27	159-106	14.02	0.58	−1	9.0	7954	301	270	311	0.69
C31	UGC7955	13.42	0.82	29	19.4	6752	372	344	412	0.76
SC29	159-018	13.05	0.62	−39	12.2	8052	469	445	451	0.82

Notes to TABLE 1

Columns (1) and (2) give our internal name and the Zwicky or UGC name of each galaxy, respectively. Column (3) is the total I-band magnitude, corrected to a distance of 7000 km s^{-1} as per the left-hand side of Eq. (1). Column (4) gives the ellipticity determined from the I-band surface photometry (see Paper I), column (5) is the position angle used for the long-slit observations, and column (6) is the semi-major axis of the isophote enclosing half the I-band light. The recession velocity in column (7) is determined from the optical data. Widths in column (8) are from the Probable Min-Max method, in column (9) using the Weighted Mean method over the range $1-2r_{1/2}$, and in column (10) we repeat the published 21-cm width (Paper I). Column (11) gives the rotation curve shape parameter defined in Eq. (2).

define a fairly robust means of quantifying the extremes of the rotation curve. We define v_{max} as that which satisfies

$$\prod_i P(v_{\mathrm{max}} > v_i) = 0.1, \qquad (1)$$

where the probabilities P are given by the standard error function if we assume that v_i has a gaussian distribution about its measured value, with dispersion σ_{v_i}. In effect we ask the following question: At what v_{max} is it likely (at the 90% level) that *some part* of the rotation curve exceeds v_{max}? A single high point on the rotation curve with a large measurement uncertainty does not unduly influence this estimator, and it is fairly insensitive to binning as well. We define an analogous v_{min} on the other side of the rotation curve and define W as the difference $v_{\mathrm{max}} - v_{\mathrm{min}}$.

5. TULLY-FISHER SCATTER

For each of the above algorithms for measuring W we evaluate the slope and scatter of the resultant TFR. As explained in Paper I, we fit to the TFR data a model of the form

$$I_{\mathrm{tot}} - 5 \log(z/0.0233) - (1 - \Omega/2 + k_I)(z - 0.0233)$$

$$= I_0 + m \log\left(\frac{W_0}{400 \text{ km s}^{-1}}\right) + a_I e. \qquad (2)$$

The left-hand side is the apparent total magnitude corrected to a standard redshift of $z = 0.0233$, or a recession velocity of 7000 km s^{-1}, assuming all galaxies to be in free Hubble expansion. Recession velocities are taken as the mean of the two arms of the rotation curve, and in general agree very well with the radio data. The k-correction factor k_I is fixed at 0.6. On the right-hand side, e is the galaxy ellipticity as determined from the I-band surface photometry, and W_0 is the measured W corrected to edge-on by the sine of the inclination angle, as described in Paper I. Note no correction is made for turbulent motion. The free parameters in the fit are I_0, m, and the inclination correction coefficient a_I.

Table 1 lists the reduced photometric data for the 25 galaxies (raw data may be found in Paper I) along with the rotation and recession velocities determined from the optical and radio data. In Table 2 we show the results of the TFR fits using widths derived by the above algorithms. Figure 2 shows an example Tully-Fisher plot produced with the Probable Min-Max widths.

The TFR scatter based on optical W data is found to be quite robust. Nearly all methods for determining W give an RMS TFR scatter of ≈ 0.14 mag. Even the simple Min-Max method works well if we consider only points with S/N > 3.5 (see Sec. *4.1*). The only algorithm noticeably less accurate than the others is the Entire Side Weighted Mean,

TABLE 2. Tully-Fisher results for various algorithms.

Algorithm	m [mag]	a_I [mag]	rms scatter [mag]
Min-Max	-5.41 ± 0.26	1.46 ± 0.20	0.140
Weighted Mean: Entire Side	-3.56 ± 0.22	1.33 ± 0.25	0.175
Weighted Mean: Outer Half	-5.47 ± 0.26	1.35 ± 0.20	0.138
Weighted Mean: $1-2r_{1/2}$	-4.95 ± 0.24	1.18 ± 0.20	0.139
Weighted Mean: $1-4r_{1/2}$	-5.08 ± 0.22	1.25 ± 0.18	0.128
Fixed Point: $1.3r_{1/2}$	-5.00 ± 0.24	1.45 ± 0.20	0.141
Probable Min-Max[a]	-5.40 ± 0.25	1.47 ± 0.25	0.135
21-cm Widths	-5.61 ± 0.18	1.42 ± 0.13	0.094

[a]This algorithm is used to produce Figs. 2 and 3

which leads us to believe that one should avoid the central portions of the rotation curve in deriving W.

Although it is not our goal to produce optical widths which best match the 21-cm widths, we do note that there are systematic differences among the different optical W estimators, and between optical and 21-cm estimates of W. As expected, those algorithms which attempt to measure the extremes of the rotation curve tend to give larger W values than those which attempt to measure the mean over some segment of the rotation curve. This can be seen by comparing columns (8) and (9) in Table 1. In galaxies which are more face-on or have smaller rotation speeds, we expect the turbulent motions to be a larger fraction of the observed velocities. If different width measurement methods have varying susceptibility to turbulent motions, this might be manifested as changes in the slope m and/or inclination correction a_I in the derived TFRs. Note, though, that the values of m and a_I in Table 2 are consistent among various algorithms, and are consistent with the values obtained using 21-cm widths.

Figure 3 plots the ratio of Probable Min-Max width to

21-cm width for all 25 galaxies as a function of inclination-corrected width W_0. No trend with W_0 is present; the optical widths are, on average, 0.96 times the 21-cm widths, with no detectable dependence upon W_0 or upon inclination. For this sample of relatively large, edge-on galaxies, the effect of turbulent velocities upon the 21-cm profiles (or perhaps the effect of extinction on the $H\alpha$ rotation curves) is small, or at least constant across the full sample.

This 25-galaxy sample also gives us little guidance on how to best treat rising rotation curves. In Fig. 1 we see that several of the galaxies have rotation curves which are still rising at the ends, particularly C19. Should we take the "true" width to be the largest observed width (using some form of Min-Max method), or something larger (an extrapolation), or something smaller (one of the weighted mean algorithms) to get the lowest TFR scatter? Which of the algorithms produces the best agreement with 21-cm widths? The near-equality of TFR scatter for all our algorithms means that we cannot offer advice on this question. The location of C19 near the top of Fig. 3 suggests that the probable Min-
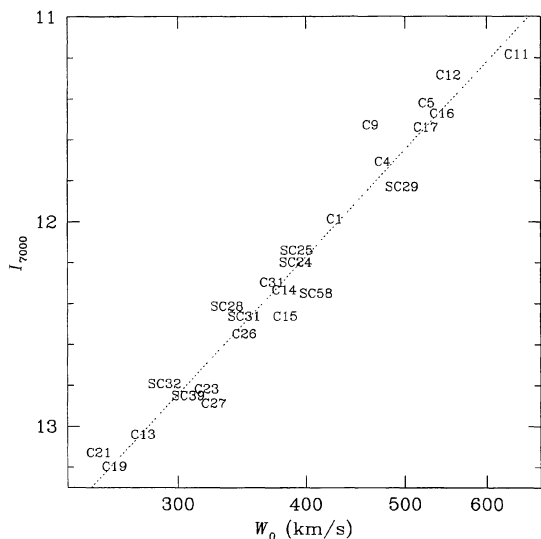

FIG. 2. Tully-Fisher relation for the 25 galaxies using widths derived from $H\alpha$ rotation curves with the "Probable Min-Max" method described in the text. Widths have been corrected to edge-on as described in Paper I, and I-band total magnitudes have been corrected to a common distance of 7000 km s^{-1}, and corrected for inclination using the value of a_I shown in Table 2. The rms deviation from the best-fit dashed line is 0.14 mag.
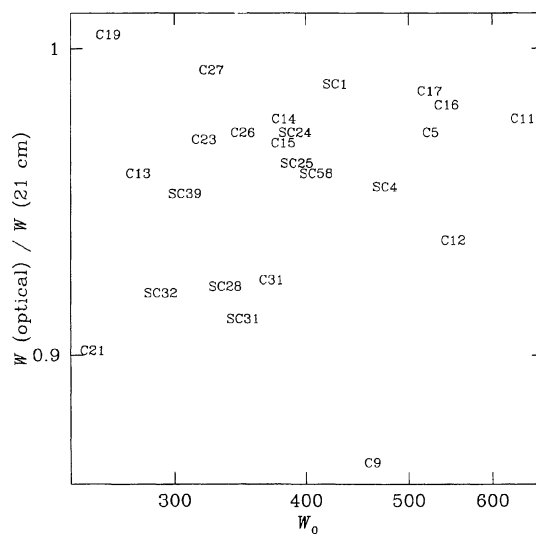
FIG. 3. Ratio of the velocity widths derived from $H\alpha$ rotation curves (using the "Probable Min-Max" method) to the 21-cm velocity widths from Paper I, plotted vs the inclination-corrected optical width. Optical widths are on average a fixed fraction (96%) of the radio widths. There is no detectable correlation between this ratio and the magnitude of the width, nor with disk inclination (latter not illustrated here).

Max W estimate of the rising rotation curve *overestimates* the rotation speed relative to 21-cm, so an extrapolation of the rising curve would make agreement worse. Even so, C19 is not an outlier from the TFR in Fig. 2. The one outlier in the optical vs 21-cm comparison, C9, is indeed the furthest outlier in the optical TFR (but is not an outlier in the 21-cm TFR). In fact most of the extra scatter in the optical TFR over the 21-cm scatter is attributable to C9. The rotation curve of C9 is, however, beautifully flat and square, so a change of algorithm would not lessen its departure from the optical TFR. Furthermore, C9 has no unusual features which would justify excluding it from our sample.

6. ROTATION CURVE SHAPES AND THIRD PARAMETERS

In principle the rotation curve provides more information than a simple width W—it has been suggested that some quantification of the *shape* of the rotation curve could be used to decrease the TFR scatter (Persic & Salucci 1990). Large homogeneous samples of rotation curves show that fast-rotating galaxies tend to have rotation curves which rise more steeply in the center than slowly-rotating galaxies, with the fastest-rotating galaxies actually having a peak in the rotation curve (PSS96).

We wish to test whether, in our limited sample, there is a trend of rotation curve shape versus W_0, or whether rotation curve shape can be used as a third parameter to reduce the TFR scatter. For each galaxy we compare the area under both arms of the rotation curve to the area under a perfectly flat rotation curve:

$$f \equiv \frac{\int_{-s_{\lim}}^{+s_{\lim}} |v(s) - v_0| \, ds}{2v_{\mathrm{rot}} s_{\lim}}. \tag{3}$$

Here s is the distance from the center of the galaxy, v_0 is the recession velocity at the center, and $\pm s_{\lim}$ are the outer bounds of the integration. The rotation velocity v_{rot} is one-half the width W, so the value of f depends upon our choice of width algorithm. If we choose $v_{\mathrm{rot}} = |v(+s_{\lim}) - v(-s_{\lim})|/2$, a solid-body rotator would have $f = 0.5$, while a perfectly flat rotation curve would have $f = 1$.

Table 1 contains the calculated value of shape parameter f for each galaxy. We determine v_{rot} using the Weighted Mean method over the range $1-4r_{1/2}$, and set $s_{\lim} = 1.3r_{1/2}$. For comparison with the study of PSS96, we note that they define R_{opt} to be the radius enclosing 83% of the light of a galaxy. For an exponential disk with scale length R_{scale}, $R_{\mathrm{opt}} = 3.2R_{\mathrm{scale}}$, while $r_{1/2} = 1.68R_{\mathrm{scale}}$, so $R_{\mathrm{opt}} = 1.9r_{1/2}$. Thus, f should be closely related to the "inner slope" defined in PSS96, or to the rotation curve slopes defined by other investigators (cf. Vogt 1994, and references therein).

In Fig. 4 we plot f vs W_0 for the 25 galaxies. There is no significant correlation, indicating that, at least in this sample, any trend of rotation curve shape vs amplitude is too weak to be detectable in individual rotation curves. This is, however, still consistent with PSS96, because: (1) we are looking at only a 2 mag range in M_I, and the PSS96 "universal" rotation curves do not change drastically over such a range, and (2) even in the PSS96 data, the shape versus W correla-
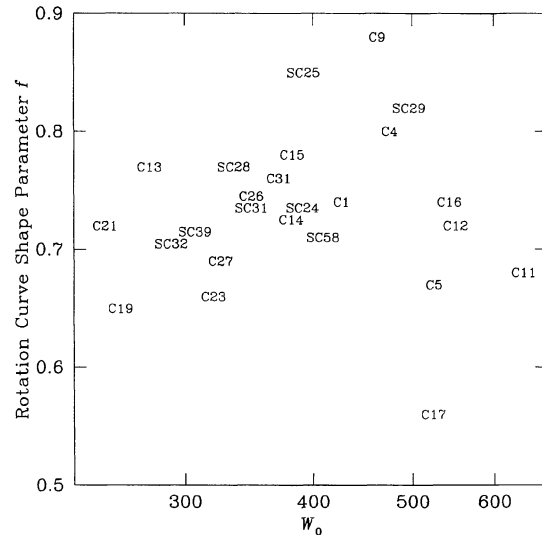

FIG. 4. Rotation curve shape vs rotation speed for the 25 galaxies. The rotation curve shape, parameterized by the quantity f defined in Eq. (2), shows no significant correlation with inclination-corrected rotation width W_0 on a galaxy-by-galaxy basis. A galaxy with solid-body rotation curve inside $1.3r_{1/2}$ would have $f = 0.5$, while a step-function rotation curve would have $f = 1$.

tion is clearest only after co-adding many rotation curves, and would not likely be detectable for 25 galaxies. Note that galaxies C11 and C17 have small f values although substantial parts of their rotation curves are flat. This is because the flat parts lie outside our integration range of $\pm 1.3r_{1/2}$; a broader integration range would extend into regions of poor S/N for some of our rotation curves and thus require undesirable extrapolation.

We also find that adding f as a parameter to the TFR fit in Eq. (2) does not reduce the resultant scatter. Thus knowledge of the steepness of the rotation curve does not, in this sample, seem to improve our ability to predict absolute I magnitude.

7. RAMIFICATIONS

We find that the rms scatter in the TFR using widths from long-slit Hα rotation curves is ≈ 0.14 mag in this sample. The TFR slope and scatter are robust under choice of algorithm for extracting the width W from the rotation curve, as long as we ignore the central section of the rotation curve and do not try to consider single points with large uncertainties (S/N<3.5 or $\sigma_v > 12$ km s^{-1}). Using F-test statistics we find that the optical scatter is greater than the 0.10 mag scatter in the 21-cm TFR for these galaxies at 95% confidence level. If we ascribe *all* of the 0.14 mag scatter in the optical-W-based TFR to errors in the W's, the TFR slope of $m \approx -5$ implies an rms error of 6% in the typical W measurement. Repeat measurements of a few galaxy rotation curves have been made, some with slit position angle intentionally placed $10°-20°$ away from the major axis, and the resultant W values are found to vary by 5% or less; we believe that measurement error in W is not the dominant

source of scatter in the optical TFR. A fit to the inverse Tully-Fisher relation gives nearly identical results because the scatter is quite small.

''Errors'' in the W values can take two forms. First, there are measurement errors, which would cause the measured value of W to differ each time we observed the galaxy. Such errors might include those due to photon statistics or poorly chosen slit position angles. Second, there could be what we will term ''astrophysical'' errors—reasons why the Hα widths do not properly measure whatever physical quantity is the underlying basis of the TFR. Examples of such cases might be velocities of H II regions which depart from the actual rotation velocity of the galaxy, or a poor choice of algorithm for measuring W so that we do not measure the relevant rotation speeds properly. Of course since we do not actually *know* what the underlying physical basis of the TFR is in any detail, we cannot address these possible errors.

The scatter in our 21-cm TFR for these 25 galaxies is extraordinarily low; most other TFR surveys find rms variations of 0.3–0.4 mag (Paper I). This could be low by a statistical fluke: our draw from the pool of either measurement errors or astrophysical errors (i.e. choice of galaxies) has been lucky. In either case, the low scatter found with Hα widths means that any *additional* errors caused by the use of optical widths is small (6% or less in W). Thus for practical purposes, we conclude that *high-quality Hα rotation curves may be used in place of 21-cm data for TFR studies, with no practical loss in precision.* This is also evident in the study of Willick *et al.* (1996), who intercompare various TFR surveys. They derive rms scatters of 0.40, 0.38, and 0.47 mag for three surveys which use 21-cm widths, and 0.38 and 0.43 mag for two surveys based primarily on Hα widths.

The scatter in the 25-galaxy sample could be very low because of some as-yet-undiscovered physical commonality that is not present in the larger TFR surveys (as the lower slope of our TFR might also suggest). In this case we could also conclude that the measurement errors on the optical W values are small, a result which is probably extendable to larger surveys. If these 25 spirals differ physically from the overall spiral galaxy population, then our results on the ro-

bustness of the W estimators and on the insignificance of rotation curve shape may not be applicable to the general spiral population.

We note also that the TFR slope and the inclination correction coefficient a_I are robust, with all optical W algorithms giving values consistent with the 21-cm values. The constancy of the TFR slope implies that Hα widths are in fixed proportion to the 21-cm widths over the range in galaxy sizes explored here. Note that our sample consists primarily of large spirals. The consistency of a_I implies that none of the algorithms is excessively subject to inclination effects. This means, for example, that the measured Hα widths are not significantly changed relative to the ''true'' widths by the effects of extinction in nearly edge-on galaxies. Since we made no corrections for turbulent velocities in either the 21-cm or the Hα data, we also infer that such corrections are not too important for the high-inclination, high-W_0 galaxies in our sample.

Finally, we note that we were unable to extract any further useful information (for TFR purposes) from the rotation curves beyond the width W. A crude measure of rotation curve shape did not improve the TFR fit, nor did we find shape to be correlated with W (and presumably galaxy mass). While such a correlation may be present when large numbers of galaxy rotation curves are co-added, or if a broader range of intrinsic galaxy sizes are studied, the galaxy-to-galaxy variations seem large enough to mask the effect for our individual objects despite the high S/N of our rotation curves.

REFERENCES

Bernstein, G. M., Guhathakurta, P., Raychaudhury, S., Giovanelli, R., Haynes, M. P., Herter, T., & Vogt, N. P. 1994, AJ, 107, 1962 (Paper I)
Courteau, S. 1992, Ph.D. thesis, University of California at Santa Cruz
Franx, M., & de Zeeuw, T. 1992, ApJ, 392, L47
Giovanelli, R., Haynes, M., Herter, T., Vogt, N., da Costa, L., Freudling, W., Salzer, J., & Wegner, G. 1997a, AJ, 113, 22
Giovanelli, R., Haynes, M., Herter, T., Vogt, N., da Costa, L., Freudling, W., Salzer, J., & Wegner, G. 1997b, AJ, 113, 53
Mathewson, D. S., Ford, V. L., & Buchhorn, M. 1992, ApJS, 81, 413

Persic, M., & Salucci, P. 1990, ApJ, 355, 44
Persic, M., Salucci, P., & Stel, F. 1996, MNRAS, 281, 27 (PSS96)
Schommer, R. A., Bothun, G. D., Williams, T. B., & Mould, J. R. 1993, AJ, 105, 97
Tully, R. B., & Fisher, J. R. 1977, A&A, 54, 661
Vogt, N. P. 1994, Ph.D. thesis, Cornell University
Willick, J. A., Courteau, S., Faber, S. M., Burstein, D., Dekel, A., & Kolatt, T. 1996, ApJ, 457, 460